Facile Access to Chain Length Dependent Termination Rate Coefficients via Reversible Addition−Fragmentation Chain Transfer (RAFT) Polymerization: Influence of the RAFT Agent Structure

Achim Feldermann,[†] Martina H. Stenzel,[†] Thomas P. Davis,[†] Philipp Vana,*[,‡] and Christopher Barner-Kowollik*[,†]

Centre for Advanced Macromolecular Design (CAMD), School of Chemical Engineering and Industrial Chemistry, The University of New South Wales, Sydney, NSW 2033, Australia, and Institut für Physikalische Chemie, Georg August Universität Göttingen,Tammannstr. 6, 37077 Göttingen, Germany

Received December 4, 2003; Revised Manuscript Received February 2, 2004

ABSTRACT: A recently developed methodology for determining chain length dependent termination rate coefficients, $\langle k_t^{i,i} \rangle$, via reversible addition−fragmentation chain transfer (RAFT) polymerizations has been extended and validated for 1-phenylethyl phenyldithioacetate (PEPDA) and 3-benzylsulfanylthiocarbonylsulfanylpropionic acid (BSPA) mediated styrene (bulk) free radical polymerizations at 80 °C. While the use of cumyl phenyldithioacetate (CPDA) enables a highly precise mapping of the chain length dependence of the termination rate coefficient, employment of PEPDA and BSPA leads to considerable information loss for short chain lengths ($i < 10$). Careful simulations demonstrate that such behavior is caused by a substantial decrease in the initial transfer effectiveness of the RAFT agents when going from CPDA to BSPA, leading to hybrid behavior between conventional and living free radical polymerization. The observed hybrid behavior is quantifiable via (overall) transfer rate coefficients for the individual RAFT agents in the preequilibrium step [CPDA ($k_{tr,R} = 5.0 \times 10^5$ L mol^{-1} s^{-1}), PEPDA ($k_{tr,R} = 2.0 \times 10^5$ L mol^{-1} s^{-1}), and BSPA ($k_{tr,R} = 1.0 \times 10^4$ L mol^{-1} s^{-1}) at 80 °C]. The underlying structural cause is the change from a tertiary (CPDA), via a secondary (PEPDA), to a primary (BSPA) leaving group in the initial RAFT agent. Further, the presented simulations open an efficient pathway for approximating overall preequilibrium transfer rate coefficients for the employed RAFT agents.

Introduction

Conventional free radical polymerization has been revolutionized by the advent of methods to control the polymerization process with respect to molecular weight and polydispersity. The three main techniques capable of inducing living behavior are nitroxide mediated polymerization (NMP),[1] atom transfer radical polymerization (ATRP),[2] and reversible addition−fragmentation chain transfer polymerization (RAFT).[3] NMP is based on the concept of reversibly capping the propagating species, utilizing the persistent radical effect.[4] Such capping reactions lower the free radical concentration and hence significantly decrease termination events. Concomitantly, the rate of polymerization is strongly decreased. The concept of ATRP is similar, but the exact mechanism of the process is still subject to scientific debate. The RAFT process, however, makes use of a different mechanism: Repeated reversible transfer events during the polymerization without—at least in principle—changing the free radical concentration[5] induce an equilibrium of dormant and living chains. In such a living system the overall rate of polymerization, R_p,[5] and the rate of the individual reaction steps remain unaltered. The specific characteristics of the RAFT process thus allow for undisturbed investigations into the termination reaction of free radical polymerizations. This notion has recently been underpinned by Prescott via a Monte Carlo approach to analyze the RAFT process.[6]

In an earlier communication we detailed a novel methodology that allows the easy determination of the chain length dependency of the termination rate coefficient.[7] The new method makes use of the direct correlation between the average chain length of the polymer chains with the monomer to polymer conversion. If the kinetic coefficients and parameters of the specific radical polymerization are known (i.e., the propagation rate coefficient, k_p, the initiator decomposition rate coefficient, k_d, and the initiator efficiency, f), time-dependent $\langle k_t \rangle$ data can be obtained via eq 1.

$$\langle k_t \rangle(t) = \frac{{k_p}^2}{(R_p(t))^2}(2f\,k_d)[I]_0 e^{-k_d t}([M]_0 - \int_0^t R_p(t)\,dt)^2 \quad (1)$$

When using a RAFT polymerization, the terminating radicals are considered to be approximately of the same chain length—ideally Poisson-distributed—at every single instant in time.[8] The time axis may hence easily be converted into a chain length axis following the simple procedure of calculating the conversion vs time data from the measured polymerization rate (represented by the integral on the right-hand side of eq 1) and assuming that the chain length of the polymer chains increases linearly with conversion. The chain length, i, may therefore be calculated as a function of time via

$$i(t) = \frac{\int_0^t R_p(t)\,dt}{[RAFT]_0} \quad (2)$$

with the initial RAFT agent concentration $[RAFT]_0$. The termination rate coefficient is now accessible by measuring the polymerization rate as a function of time in a RAFT agent mediated polymerization, assuming that all terminating chains have the same chain length. This

* To whom correspondence should be addressed. E-mail: camd@unsw.edu.au.
[†] The University of New South Wales.
[‡] Georg August Universität Göttingen.

10.1021/ma0358428 CCC: $27.50
Published on Web 03/09/2004

Scheme 1. RAFT Agents Employed in the Current Study: Cumyl Phenyldithioacetate (CPDA), 1-Phenylethyl Phenyldithioacetate (PEPDA), and 3-Benzylsulfanylthiocarbonylsulfanylpropionic Acid (BSPA)

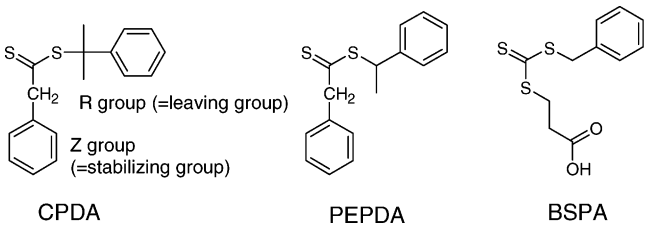

Scheme 2. Basic Reactions Describing the Reversible Addition−Fragmentation Chain Transfer (RAFT) Process[a]

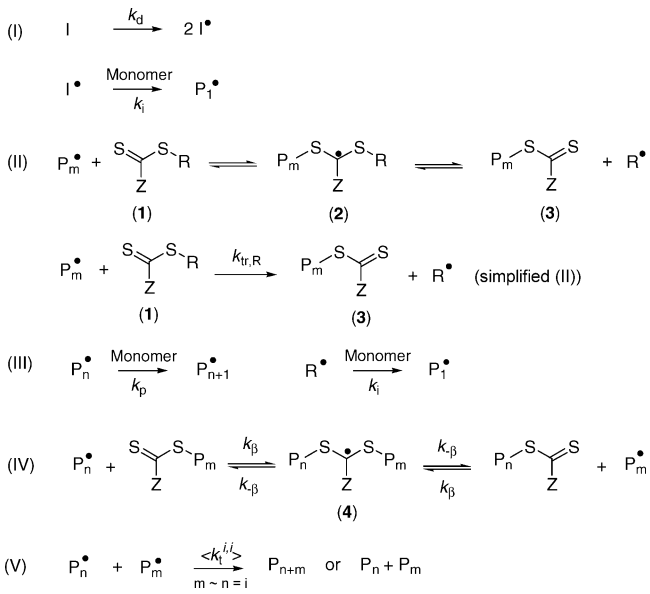

[a] For a detailed explanation see text.

task is easily realized by isothermal DSC which directly determines the polymerization rate by monitoring the reaction heat. The chain length dependence and the absolute value of k_t may therefore be accessed via one experiment. It should be noted that the presented methodology does not control the weight fraction of the polymer in the system.

In our previous study, we demonstrated that the above methodology can be successfully applied to map out the chain length dependency of the termination rate coefficient in the free radical polymerization of styrene using a RAFT agent carrying a destabilizing Z-moiety, i.e., cumyl phenyldithioacetate (CPDA, see Scheme 1). In the present study we wish to report data on the effect of the RAFT agent structure on the obtained chain length dependence. We will demonstrate that the structural design of the RAFT agent is essential for obtaining reliable termination rate coefficient data. Three RAFT agents, i.e., cumyl phenyldithioacetate (CPDA), 1-phenylethyl phenyldithioacetate (PEPDA), and 3-benzylsulfanylthiocarbonylsulfanylpropionic acid (BSPA), were used for this purpose.

The basic mechanism of the RAFT process is depicted in Scheme 2. Reaction I represents the initiator decomposition process, which proceeds with a rate coefficient k_d. The ability of the generated radicals to initiate macromolecular growth is quantified by the initiator efficiency, f, and the initiation rate coefficient, k_i. Both k_d and f are available from the literature over a wide range of temperatures.[9,10] The initiation rate coefficient k_i is generally very large[11] and can hence considered to be kinetically not relevant, since the initiator fragment radicals are nearly instantaneously transformed into growing macroradicals. Reaction I of an initiator-derived radical, I$^\bullet$, with monomer is therefore assumed to be approximately 5 times faster than the long chain propagation rate coefficient, k_p. Some evidence has recently been put forward toward a chain length dependence of the propagation rate coefficient.[12−15] However, this effect is currently not fully understood, and we therefore used a chain length independent k_p value in our study. The RAFT preequilibrium (II), which involves the initial RAFT agent (**1**) and the macroRAFT radical (**2**), may be simplified to a transfer reaction with an overall transfer rate coefficient, $k_{tr,R}$. It goes without saying that $k_{tr,R}$ is a composite of the rate coefficients governing the preequilibrium (II). The reaction steps given in (III) represent the propagation and reinitiation reactions. The core of the RAFT process is the "main" equilibrium (IV). The two rate coefficients k_β and $k_{-\beta}$ control the position of the equilibrium: k_β (corresponding to the addition step) controls the bimolecular reaction between free macroradicals and polymeric RAFT-agent, which leads to the formation of the macroRAFT radical (**4**). $k_{-\beta}$ can be associated with the (average) lifetime of the macroRAFT radical. Finally, the reaction step (V) describes bimolecular (chain length dependent) termination of free macroradicals, which leads to the formation of "dead" polymeric product that is no longer capable of chain extension. Not shown in Scheme 2 are termination reactions between free macroradicals and initiator-derived radicals, I$^\bullet$, as well as initial RAFT agent-derived radicals, R$^\bullet$. There is an ongoing debate about the exact nature of the RAFT process, and various research groups have attempted to obtain information on the mechanism and kinetics of the process, either through the interpretation of dynamic kinetic and molecular weight data employing computer-based modeling strategies,[16−20] or the direct observation of intermediate species,[21−24] or through high-level ab initio molecular orbital calculations.[25] The scientific debate has focused particular attention on the fate of the so-called intermediate macroRAFT radicals (species **2** and **4**, Scheme 2) that are formed in the preequilibrium and main equilibrium of the RAFT process.[26] Evidence has been put forward for a relatively long lifetime, τ, of the intermediate radicals in cases where high stabilization of such radicals is possible (i.e., τ on the order of seconds),[16−19,24,25,27] as well as for a cross-termination reaction (either reversible[27,28] or irreversible[21,22]) of the intermediate radicals with themselves or with propagating chains. However, broad agreement exists that in RAFT systems that show neither rate retardation (i.e., a decreased rate of polymerization in comparison to the corresponding non-RAFT system) nor inhibition (no polymerization activity in the initial phase of the polymerization in comparison to the non-RAFT system) phenomena, the mechanism depicted in Scheme 2 is an adequate representation of the physical reality.

The mechanism shown in Scheme 2, however, can still lead to non- or semiliving behavior of the polymerization system, if the associated rate coefficients are not appropriate. For example, if the preequilibrium of the RAFT process (reaction step II in Scheme 2) is not completed within a certain time frame, a hybrid behav-

ior between conventional and living free-radical polymerization is observed.[17] Such a hybrid behavior results in cases when the transfer rate coefficient for the simplified transfer reaction, $k_{tr,R}$, describing the RAFT preequilibrium is too low compared to the propagation rate coefficient, k_p. The result is a rapid increase of the molecular weight at the very beginning of the polymerization process followed by a linear increase up to high monomer to polymer conversions. Hybrid behavior in a RAFT system has been previously described by the CAMD group for the CPDA mediated methyl methacrylate (MMA) free radical polymerization.[17] The aim of the present study is to demonstrate that even RAFT agents that do not display rate retardation and inhibition phenomena with a particular monomer can only be employed for chain length dependent termination rate measurements, if they do not induce hybrid transfer behavior. To elucidate the consequences of hybrid transfer behavior on our methodology for arriving at chain length dependent termination rate coefficients, careful simulations via the PREDICI program package were carried out. Incidentally, the presented simulation approach may be used to arrive at (overall) $k_{tr,R}$ values for the RAFT preequilibrium in a reverse engineering fashion.

Experimental Section

Materials. Styrene (Aldrich, 99%) was purified by passing over a column of basic alumina prior to use. Cumyl phenyldithioacetate (CPDA) was prepared as described earlier,[17] using *n*-hexane as the solvent. 1-Phenylethyl phenyldithioacetate (PEPDA) was prepared via the same method as used for CPDA; however α-methylstyrene was replaced by styrene (see ref 29). The purity of the RAFT agents was close to 99% as verified by ^{1}H NMR analysis and elemental analysis. 3-Benzylsulfanylthiocarbonylsulfanylpropionic acid (BSPA) was obtained via the method described in detail in ref 30. 2,2′-Azobis(isobutyronitrile) (AIBN, Aldrich, 99%) was recrystallized twice from ethanol prior to use.

Polymerizations (DSC). Solutions of monomer with AIBN and CPDA, BSPA, or PEPDA ($[\text{Initiator}]_0 = 1.7 \times 10^{-2}$ mol L^{-1}, $[\text{RAFT}]_0 = 1.1 \times 10^{-2}$ mol L^{-1}) were thoroughly deoxygenized in a nitrogen stream and handled inside a glovebox filled with dry nitrogen gas (99.99% pure) all the time. Exactly weighed amounts of sample (15−25 mg) were loaded to alumina pans that were sealed with alumina lids. The polymerization heat was determined isothermally at 80 °C via measuring the heat flow vs an empty sample pan in a differential scanning calorimeter (Perkin-Elmer DSC 7 with a TAC 7/DX thermal analysis instrument controller). The DSC instrument was calibrated with a standard indium sample of known mass, melting point temperature, and known associated enthalpy change. All DSC monitored polymerization runs were performed in duplicate. The rate of polymerization, R_p, was calculated using literature values for the heat of polymerization of styrene.[31]

Polymerizations (General). Stock solutions of initial RAFT agent and AIBN concentrations identical to those used in the DSC experiments described above were transferred to five individual ampules, which were thoroughly deoxygenated by purging with nitrogen gas for approximately 15 min. The sealed ampules were subsequently placed in a thermostated oil bath at 80 °C and removed after 0.5, 1, 2, 4, and 6 h. The reactions were stopped via cooling the solutions in an ice bath followed by the addition of a small amount of hydroquinone. The polymer was isolated by evaporating off the residual styrene—initially in a fume cupboard to remove the bulk of the liquid and then in a vacuum oven at 30 °C. Final conversions were measured gravimetrically.

Molecular Weight Analysis. Molecular weight distributions were measured via size exclusion chromatography (SEC) on a Shimadzu modular system, comprising an auto injector, a Polymer Laboratories 5.0 μm bead size guard column (50 × 7.5 mm), followed by three linear PL columns (10^5, 10^4, and 10^3 Å) and a differential refractive index detector (Shimadzu RID-10A). The eluent was tetrahydrofuran (THF) at 40 °C with a flow rate of 1 mL min^{-1}. The system was calibrated using narrow polystyrene standards ranging from 500 to 10^6 g mol^{-1}.

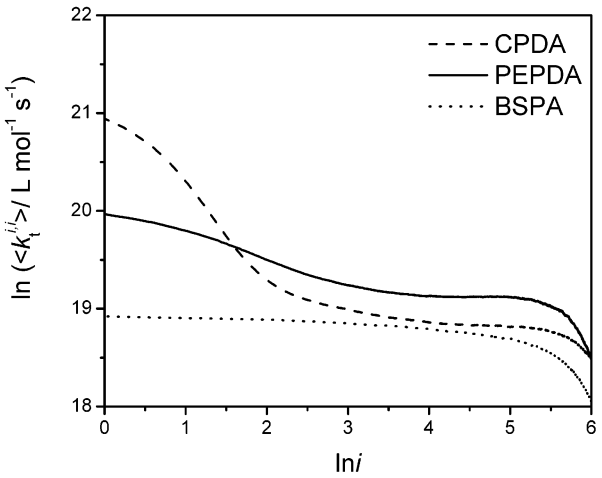

Figure 1. Double-logarithmic plots of $\langle k_t^{i,i} \rangle$ vs i, evaluated from experimental time-resolved R_p data according to the procedure described in the text at 80 °C for CPDA, PEPDA, and BSPA mediated styrene free radical polymerizations.

Simulations. All simulations have been carried out using the program package PREDICI, version 5.36.4a, on a Pentium IV (HT), 2.6 GHz IBM-compatible computer.

Results and Discussion

Bulk polymerizations of styrene were performed at 80 °C using AIBN as the free radical initiator and mediated by CPDA, PEPDA, and BSPA. The rate of polymerization was monitored on-line via isothermal DSC and was subsequently transformed into $\langle k_t^{i,i} \rangle$ vs i plots according to the procedure described in the Introduction and given in greater detail in ref 7. Equation 1 shows that values for k_p, f, and k_d are necessary to successfully calculate $\langle k_t^{i,i} \rangle$. These parameters are well established for the AIBN-initiated bulk polymerization of styrene, and the following set of kinetic coefficients were used: $k_p = 663$ L mol^{-1} s^{-1} (ref 32), $f = 0.713$ (ref 10), and $k_d = 1.36 \times 10^{-4}$ L mol^{-1} s^{-1} (ref 33). Figure 1 shows the obtained ln $\langle k_t^{i,i} \rangle$ vs ln i plots for the three RAFT agents.

Inspection of Figure 1 shows that the characteristic "three region" chain length dependence of k_t at small chain length ($1 < i < 10$) is well represented in the CPDA mediated system,[7] whereas the BSPA mediated system yields a very different dependence of the termination rate coefficient on the chain length i, i.e., almost no dependence of k_t on the chain length for $i < 100$. For chain lengths exceeding $i > 100$ the obtained $\langle k_t^{i,i} \rangle$ value shows (for all three RAFT agents) a significant decrease. This drop in k_t is partly due to the conversion dependence of the termination reaction (or—more precisely—its dependence on the weight fraction of polymer), which becomes significant above ∼30% in styrene bulk polymerizations.[34] The linkage between chain length and conversion in living free radical polymerizations does not allow for the separation of these two influences on k_t. However, the $\langle k_t \rangle$ is believed to be almost constant up to a monomer to polymer conversion of ∼30% (in the absence of RAFT agent), hence validating the above

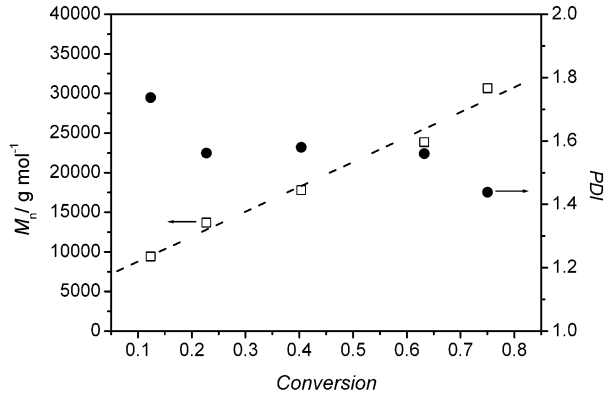

Figure 2. Experimentally obtained number-average molecular weights, M_n (open squares, left axis, dotted line indicates least-squares linear fit), and polydispersity indices, PDI (full circles, right axis), as a function of monomer conversion for BSPA mediated styrene polymerizations carried out at 80 °C.

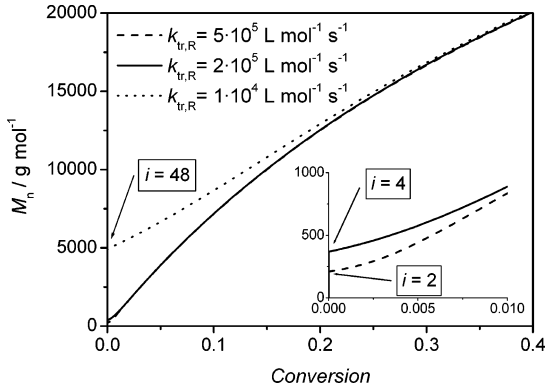

Figure 3. Simulated number-average molecular weight, M_n, as a function of monomer conversion for different values of the (overall) transfer rate coefficient, $k_{tr,R}$, governing the RAFT preequilibrium. The simulations have been carried out via the program package PREDICI using the coefficients given in Table 1. The intercept with the molecular weight axis is given by the chain length, i ($i \neq 0$ indicates that hybrid behavior is involved).

determination of the chain length dependence of $\langle k_t^{i,i} \rangle$. The PEPDA mediated system shows a behavior that is intermediate in nature to both the CPDA and the BSPA systems. The initial $\langle k_t^{1,1} \rangle$ value in the PEPDA system lies somewhat lower than that obtained in the CPDA system, but the characteristic "three region" shape[7,35] of the chain length dependence of k_t is still clearly visible. Theoretically (see discussion below and Figure 4), the value for the termination rate coefficient at larger chain lengths should be identical and independent of the RAFT agent employed. The observable differences are due to experimental scatter. We estimate the absolute level of k_t to be accurate within ±30%.

The key toward understanding the observed (apparent) chain length dependencies of the termination rate coefficient for the different RAFT systems lies in the evolution of the molecular weight distributions with monomer to polymer conversion. Only one of the observed chain length dependencies of the termination rate coefficient can be considered a representation of the physical reality; i.e., the depicted chain length axis, ln i, in Figure 1 is only valid for the CPDA mediated process (see below). Figure 2 depicts the experimentally obtained number-average molecular weight, M_n, vs conversion plot for a BSPA mediated styrene free radical polymerization at 80 °C. The initial RAFT agent and

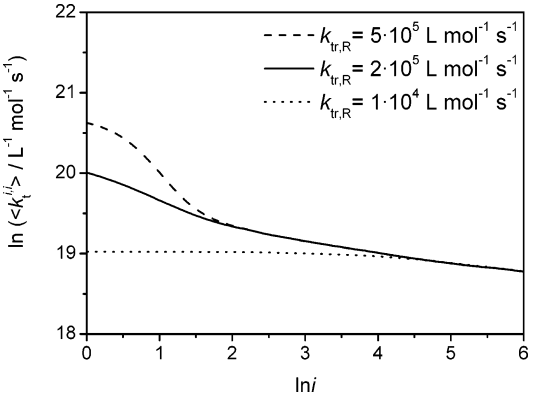

Figure 4. Double-logarithmic plots of $\langle k_t^{i,i} \rangle$ vs i, evaluated from simulated time-resolved R_p data (using the coefficients from Table 1) according to the procedure described in the text.

AIBN concentrations were identical to those used in the corresponding DSC experiments. Clearly, the molecular weight increases in a stepwise fashion (i.e., the M_n vs conversion graph does not pass through the origin) at extremely low monomer to polymer conversions and subsequently shows a linear dependence on conversion.

The polydispersity indices, PDI, of the generated molecular weight distributions are relatively high in the earlier stages of the polymerization but narrow considerably for higher conversions. Such high PDIs have been reported earlier for RAFT systems displaying hybrid behavior.[17] The reasons for the sudden increase in molecular weight and the initially high polydispersities are associated with an overall small transfer rate coefficient, $k_{tr,R}$, for the simplified form of the preequilibrium. We have demonstrated in a previous study that an insufficiently high $k_{tr,R}$ in the preequilibrium leads to hybrid behavior between living and conventional free radical polymerization.[17] To clarify whether such hybrid behavior can cause the observed (apparent) chain length dependencies given in Figure 1, simulations of the number-average molecular weight, M_n, the monomer to polymer conversion as a function of reaction time, and the rate of polymerization were carried out via the PREDICI program package, following a simulation strategy described earlier.[18] The specific implementation of the reaction sequences given in Scheme 2 into the PREDICI program package has been detailed in refs 16 and 36. In the simulations, the full distribution of all polymeric radicals is considered at any point in time.

The simulated polymerization rate vs time data were subsequently subjected to our novel analysis method (see eqs 1 and 2). A chain length dependent termination rate coefficient (for all macroradical/macroradical terminations) was introduced into the simulations based on the findings of our earlier communication, which employed CPDA as mediating agent. The findings of our earlier communication with respect to the chain length dependence of the termination rate coefficient were in excellent agreement with previous studies.[37−39] For the present study of RAFT agent influences on the new method, we consequently used the chain length dependent termination rate coefficient obtained from the CPDA system.[7] The $\langle k_t^{i,i} \rangle$ vs i functionality was implemented as a direct data pair file into the PREDICI program package.[40] It should be noted that only $\langle k_t^{i,i} \rangle$ values up to chain length $i = 50$ were included to avoid implementation of the overlying conversion dependency of the termination rate coefficient.[7] Instead, the $\langle k_t^{i,i} \rangle$ vs i data were extended to decrease with the widely accepted

Table 1. Set of Rate Coefficients Used for the Simulation of the Number-Average Molecular Weight, M_n, and the Monomer to Polymer Conversion in the RAFT Mediated Free Radical Bulk Polymerization of Styrene at 80 °C[a]

k_d/s^{-1}	k_p	f	k_i	k_β	$k_{-\beta}/s^{-1}$	$k_{tr,R}$
1.36×10^{-4}	663	0.713	3200	5.0×10^5	1×10^5	see Figures 3−5

[a] All data are taken from ref 7 and the literature cited therein. All rate coefficients are given in L mol^{-1} s^{-1} unless otherwise indicated.

functionality $k_t^{i,i} = k_t^{i=50} \cdot 50^{+0.16} \cdot i^{-0.16}$, according to previously published data.[35] The additional simulation input parameters were $k_{tr,R} = 1 \times 10^4$ (BSPA), 2×10^5 (PEPDA), and 5×10^5 L mol^{-1} s^{-1} (CPDA), $k_p = 663$ L mol^{-1} s^{-1}, $k_\beta = 5 \times 10^5$ L mol^{-1} s^{-1}, $k_{-\beta} = 1 \times 10^5$ s^{-1}, $k_d = 1.36 \times 10^{-4}$ s^{-1}, $[\text{Initiator}]_0^{\text{simul}} = [\text{Initiator}]_0^{\text{exp}} = 1.7 \times 10^{-2}$ mol L^{-1}, $[\text{RAFT}]_0^{\text{simul}} = [\text{RAFT}]_0^{\text{exp}} = 1.1 \times 10^{-2}$ mol L^{-1}, and $[M]_0 = 8.73$ mol L^{-1} (see also Table 1). Side reactions, such as intermediate storage effects and intermediate termination reactions, are not included, and fragmentation (described by $k_{-\beta}$) of the intermediate macroRAFT radical was assumed to be fast for all employed RAFT agents. As long as $k_{-\beta}$ is large enough, radical storage effects will not play a prominent role, and its absolute value has little influence on the simulation outcome. The value for $k_{-\beta}$ given in ref 17 (2.7×10^{-1} s^{-1}) for the CPDA/styrene system may be interpreted as a lower bound as to where (almost) no retardation is observable. The RAFT process is a powerful tool for kinetic investigations into free radical polymerizations when judiciously choosing the RAFT agent such that it does not induce significant rate retardation effects. For CPDA,[17] PEPDA,[41] and BSPA[42] mediated bulk styrene polymerization no rate retardation (and inhibition) effects have been observed.

Figure 3 shows the simulated evolution of the number-average molecular weight, M_n, vs monomer conversion for the CPDA, PEPDA, and BSPA mediated styrene polymerizations at 80 °C. Inspection of Figure 3 clearly shows that hybrid behavior is observed for BSPA and to some extent for PEPDA (see enlargement), with (almost) no hybrid behavior discernible for the CPDA mediated system. The figure also indicates the extent of the initial increase of the molecular weight in terms of the (average) polymer chain length at a monomer to polymer conversion of 10^{-3}%. While for BSPA a sudden increase in molecular weight to approximately 48 styrene units is calculated, PEPDA only effects an increase to 4 units, while CPDA leads to almost perfect living behavior ($i^{\text{initial}} = 2$). The underlying chemical reason for the change in the simulated (and implicitly observed, see Figure 1) M_n vs conversion evolution is associated with the fact that CPDA carries a tertiary (= cumyl) leaving group, whereas PEPDA carries a secondary (= 1-phenylethyl) and BSPA a primary (= benzyl) leaving group (see Scheme 1). The RAFT preequilibrium (reaction step II in Scheme 2) lies more to the right-hand side when a RAFT agent with a tertiary leaving group is selected than in cases where a secondary or primary group is used. A tertiary leaving group forms a more stable radical than a secondary or primary one, thus effecting a faster fragmentation of the intermediate RAFT radical (species **2** in Scheme 2) to the right-hand side. A less effective leaving group will delay the complete conversion of initial RAFT agent (**1**) into the macroRAFT agent (**3**). Consequently, the establishment of the main RAFT equilibrium (reaction step IV in Scheme 2) is also delayed, leading to uncontrolled macromolecular growth up to significant chain lengths before the RAFT process can effectively control the chain equilibration.[17] The resulting net effect is that the molecular weight rapidly increases to a certain value at which living free radical behavior with a linear evolution of molecular weight with conversion sets in. The hybrid behavior seen in Figures 2 and 3 is thus caused by a considerable difference in the (overall) transfer rate coefficients of the RAFT preequilibrium. It should be noted that when going from CDPA or PEPDA to BSPA, not only the R group is altered but also the Z group changes. However, the employed Z group has been reported to not stabilize the resulting intermediate macroRAFT radicals,[42] and we assume it is similar in this respect to the benzyl Z group of CPDA and PEPDA.

The transfer rate coefficients, $k_{tr,R}$, used in the simulated data of Figure 3 were obtained by systematic variation of their value until the simulated ln $\langle k_t^{i,i} \rangle$ vs ln i functionalities given in Figure 4 approximately matched those obtained experimentally (see Figure 1). The values for $k_{tr,R}$ given in Figures 3 and 4 reflect the optimum numbers for $k_{tr,R}$ in the cases of CPDA, PEPDA, and BSPA. A similar trend for (overall) chain transfer constants when going from tertiary, via secondary, to primary leaving groups has recently been reported by the CSIRO group for RAFT mediated methyl methacrylate (MMA) free radical polymerizations.[43] It is gratifying to note that the experimentally obtained molecular weight evolution of the BSPA mediated styrene bulk polymerization given in Figure 2 matches the one obtained by the simulation/data fitting process reasonably well. It should however be stressed that the $k_{tr,R}$ values reported for the simplified preequilibrium are of an approximate nature only, and it is estimated that they are beset with an error of ±30%, which is mainly due to the scatter in the experimental data sets.

It is evident from the simulated ln $\langle k_t^{i,i} \rangle$ vs ln i plots that the structurally caused variation (i.e., going from a tertiary to a primary leaving group) of $k_{tr,R}$ effects the observed (apparent) chain length dependencies of the termination rate coefficient. The hybrid nature of the BSPA mediated styrene polymerizations causes the short chain lengths ($i < 48$) to be omitted by jumping to a certain average molecular weight instantaneously. A similar—although far less pronounced—effect can be observed in the PEPDA system, where chain lengths smaller than four ($i < 4$) are omitted. The experimentally obtained chain length dependencies for these two RAFT agents thus only show a reduced or—in effect—later part of the termination rate coefficient vs chain length plot. The simulated ln $\langle k_t^{i,i} \rangle$ vs ln i plots given in Figure 4 do, of course, not show any conversion dependence of the termination rate coefficient (i.e., a decrease of the overall k_t values at large chain length or high monomer to polymer conversions), as such a dependence has not been implemented into the simulations. The simulated ln $\langle k_t^{i,i} \rangle$ vs ln i plots exhibit a slope slightly smaller than 0.16 at ln $i > 4$ (see above), i.e., for chain lengths larger than $i = 50$ ($k_t^{i,i} = k_t^{i=50} \cdot 50^{+0.16} \cdot i^{-0.16}$). This result is in agreement with numbers reported earlier[7] and is a reflection of the fact that the simulation uses the full macroradical distributions.

It is worthwhile to plot the resulting (simulated) conversion vs time curves for the three RAFT systems. As can be seen from Figure 5, the variation in the

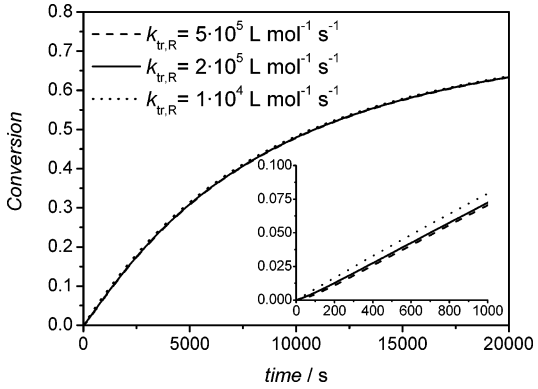

Figure 5. Simulated monomer to polymer conversion as a function of reaction time for different values of the overall transfer rate coefficient, $k_{tr,R}$, governing the RAFT preequilibrium. The simulations have been carried out via the program package PREDICI using the coefficients given in Table 1 with a preselected chain length dependent termination rate coefficient as described in the text.

conversion vs time profiles due to the change in the (overall) transfer rate coefficients is minute (see inset in Figure 5). Nevertheless, if the conversion−time curves are differentiated to yield rate of polymerization vs time plots and subsequently subjected to analysis via eq 1, the graphs given in Figure 4 result. Such minute differences in the conversion vs time plots will only be registered by either highly accurate spectroscopic techniques such as Fourier transform near-infrared (FT-NIR) spectroscopy or on-line DSC as employed in the present study.

Conclusions

In the present paper we have conclusively shown that the RAFT agents for use in our novel methodology to arrive at chain length dependent termination rate coefficients have to be judiciously selected. Particular attention needs to be paid to the rapid equilibration of chains via a fast preequilibrium step in the RAFT process. We advise choosing RAFT agents that do not display hybrid behavior between conventional and living free radical polymerization, as this phenomenon will severely affect the chain length axis. Cumyl phenyldithioacetate (CPDA) is excellently suited to study the chain length dependency of the termination rate coefficient, whereas caution with regard to the validity of the *x*-axis in the resulting ln $\langle k_t^{i,i} \rangle$ vs ln *i* plots when employing 1-phenylethyl phenyldithioacetate (PEPDA) and 3-benzylsulfanylthiocarbonylsulfanylpropionic acid (BSPA) has to be exercised. Further, we demonstrated that it is feasible to estimate (overall) chain transfer rate coefficients for the preequilibrium of the RAFT process for the three studied RAFT agents in styrene bulk free radical polymerizations. The transfer rate coefficients decrease in the order CPDA > PEPDA > BSPA, in accordance with the radical stability of the associated leaving groups of the individual RAFT agents.

Acknowledgment. The authors acknowledge financial support from the Australian Research Council (ARC). T.P.D. acknowledges receipt of an Australian Professorial Fellowship. The authors thank Dr. Markus Busch for his expert and friendly advice on all matters regarding the PREDICI program package.

References and Notes

(1) Matyjaszewski, K. *Controlled/Living Radical Polymerization—Progress in ATRP, NMP and RAFT*; American Chemical Society: Washington, DC, 2000; Vol. 768. (b) Hawker, C. J.; Bosman, A. W.; Harth, E. *Chem. Rev.* **2001**, *101*, 3661−3688.
(2) Wang, J. S.; Matyjaszewski, K. *J. Am. Chem. Soc.* **1995**, *117*, 5614−5615. (b) Haddleton, D. M.; Crossman, M. C.; Dana, B. H.; Duncalf, D. J.; Heming, A. M.; Kukulj, D.; Shooter, A. J. *Macromolecules* **1999**, *32*, 2110−2119.
(3) Mayadunne, R. T. A.; Rizzardo, E.; Chiefari, J.; Chong, Y. K.; Moad, G.; Thang, S. H. *Macromolecules* **1999**, *32*, 6977−6980. (b) Moad, G.; Chiefari, J.; Chong, Y. K.; Krstina, J.; Mayadunne, R. T. A.; Postma, A.; Rizzardo, E.; Thang, S. H. *Polym. Int.* **2000**, *49*, 993−1001. Chong, Y. K.; Le, T. P. T.; Moad, G.; Rizzardo, E.; Thang, S. H. *Macromolecules* **1999**, *32*, 2071−2074.
(4) Fischer, H. *Chem. Rev.* **2001**, *101*, 3581−3610.
(5) The statement that the radical concentration is unaltered in RAFT systems is strictly speaking only true for chain length independent termination kinetics. However, a nonretarding RAFT system comes very close to the situation of an unchanged radical population compared to the corresponding conventional polymerization. An identical approximation is true for the rate of polymerization. Nevertheless, it must be stated that the use of the calculated radical concentration (from the conventional system) constitutes an assumption.
(6) Prescott, S. W. *Macromolecules* **2003**, *36*, 9608−9621.
(7) Vana, P.; Davis, T. P.; Barner-Kowollik, C. *Macromol. Rapid Commun.* **2002**, *23*, 952−956.
(8) Müller, A. H. E.; Yan, D.; Litvinenko, G.; Zhuang, R.; Dong, H. *Macromolecules* **1995**, *28*, 7335−7338. (b) Müller, A. H. E.; Zhuang, R.; Yan, D.; Litvinenko, G. *Macromolecules* **1995**, *28*, 4326−4333. (c) Litvinenko, G.; Müller, A. H. E. *Macromolecules* **1997**, *30*, 1253−1266.
(9) Moad, G.; Rizzardo, E.; Solomon, D. H.; Johns, S. R.; Willing, R. I. *Makromol. Chem., Rapid Commun.* **1984**, *5*, 793−798.
(10) Buback, M.; Huckestein, B.; Kuchta, F.-D.; Russell, G. T.; Schmid, E. *Macromol. Chem. Phys.* **1994**, *195*, 2117−2140.
(11) Fischer, H.: Radom, L. *Angew. Chem., Int. Ed.* **2001**, *40*, 1340−1371.
(12) Olaj, O. F.; Vana, P.; Zoder, M.; Kornherr, A.; Zifferer, G. *Macromol. Rapid Commun.* **2000**, *21*, 913−920.
(13) Heuts, J. P. A.; Gilbert, R. G.; Radom, L. *Macromolecules* **1995**, *28*, 8771−8781 and literature cited therein.
(14) Beuermann, S. *Macromolecules* **2002**, *35*, 9300−9305.
(15) Willemse, R. X. E.; Staal, B. B. P.; van Herk, A. M.; Pierik, S. C. J.; Klumperman, B. *Macromolecules* **2003**, *36*, 9797−9803.
(16) Barner-Kowollik, C.; Quinn, J. F.; Morsley, D. R.; Davis, T. P. *J. Polym. Sci., Polym. Chem.* **2001**, *39*, 1353−1365.
(17) Barner-Kowollik, C.; Quinn, J. F.; Nguyen, T. L. U.; Heuts, J. P. A.; Davis, T. P. *Macromolecules* **2001**, *34*, 7849−7857.
(18) Vana, P.; Davis, T. P.; Barner-Kowollik, C. *Macromol. Theory Simul.* **2002**, *11*, 823−835.
(19) Perrier, S.; Barner-Kowollik, C.; Quinn, J. F.; Vana, P.; Davis, T. P. *Macromolecules* **2002**, *35*, 8300−8306.
(20) Zhang, M.; Ray, W. H. *Ind. Eng. Chem. Res.* **2001**, *40*, 4336−4352.
(21) Monteiro, M. J.; de Brouwer, H. *Macromolecules* **2001**, *34*, 349−352.
(22) Kwak, Y.; Goto, A.; Tsujii, Y.; Murata, Y.; Komatsu, K.; Fukuda, T. *Macromolecules* **2002**, *35*, 3026−3029.
(23) Calitz, F. M.; McLeary, J. B.; McKenzie, J. M.; Tonge, M. P.; Klumperman, B.; Sanderson, R. D. *Macromolecules* **2003**, *36*, 9687−9690.
(24) Ah Toy, A.; Vana, P.; Davis, T. P.; Barner-Kowollik, C. *Macromolecules* **2004** *37*, 744−751.
(25) Coote, M. L.; Radom, L. *J. Am. Chem. Soc.* **2003**, *125*, 1490−1491.
(26) Barner-Kowollik, C.; Coote, M. L.; Davis, T. P.; Radom, L.; Vana, P. *J. Polym. Sci., Polym. Chem.* **2003**, *41*, 2828−2832. Wang, A. R.; Zhu, S.; Kwak, Y.; Goto, A.; Fukuda, T.; Monteiro, M. S. *J. Polym. Sci., Polym. Chem.* **2003**, *41*, 2833−2839.
(27) Vana, P.; Quinn, J. F.; Davis, T. P.; Barner-Kowollik, C. *Aust. J. Chem.* **2002**, *55*, 425−431.
(28) Monteiro, M. J.; Bussels, R.; Beuermann, S.; Buback, M. *Aust. J. Chem.* **2002**, *55*, 433−437.
(29) Quinn, J. F.; Rizzardo, E.; Davis, T. P. *Chem. Commun.* **2001**, 1044−1046.
(30) Jesberger, M.; Barner, L.; Stenzel, M. H.; Malmström, E.; Davis, T. P.; Barner-Kowollik, C. *J. Polym. Sci., Polym. Chem.* **2003**, *41*, 3847−3861.
(31) Bywater, S.; Worsfold, D. J. *J. Polym. Sci.* **1962**, *58*, 571−579.

(32) Buback, M.; Gilbert, R. G.; Hutchinson, R. A.; Klumperman, B.; Kuchta, F.-D.; Manders, B. G.; O'Driscoll, K. F.; Russell, G. T.; Schweer, J. *Macromol. Chem. Phys.* **1995**, *196*, 3267−3280.
(33) Breitenbach, J. W.; Schindler, A. *Monatsh. Chem.* **1957**, *88*, 810−821.
(34) Buback, M.; Kuchta, F.-D. *Macromol. Chem. Phys.* **1997**, *198*, 1455−1480.
(35) Barner-Kowollik, C.; Vana, P.; Davis, T. P. In *Handbook of Radical Polymerization*, 1st ed.; Davis, T. P., Matyjaszewski, K., Eds.; Wiley-Interscience: New York, 2002; p 187.
(36) Wulkow, M.; Busch, M.; Davis, T. P.; Barner-Kowollik, C. *J. Polym. Sci., Polym. Chem.* **2004** *42*, 1441−1448.
(37) Beckwith, A. J. L.; Griller, D.; Lorand, J. P. In *Landolt-Börnstein, Numerical Data and Functional Relationships in Science and Technology, New Series*; Fischer, H., Ed.; Springer-Verlag: Berlin, 1984; Vol. 13, Part a, Chapter 1.
(38) Olaj, O. F.; Vana, P. *J. Polym. Sci., Polym. Chem.* **2000**, *38*, 697−705.
(39) Buback, M.; Busch, M.; Kowollik, C. *Macromol. Theory Simul.* **2000**, *9*, 442−452.
(40) Implementation as a direct data file pair implies that to each (discrete) chain length a value for the termination rate coefficient is assigned in a table. In the course of the simulation, the current average radical chain length is calculated, and the corresponding termination rate coefficient is selected from the data file table. Thus, termination rate coefficients for identical radical chain lengths are deduced; i.e., each (average) chain length is assigned to a $k_t^{i,i}$.
(41) Lansalot, M.; Davis, T. P.; Heuts, J. P. A. *Macromolecules* **2002**, *35*, 7582−7591.
(42) Stenzel, M. H.; Davis, T. P. *J. Polym. Sci., Polym. Chem.* **2002**, *40*, 4498−4512.
(43) Chong, Y. K. (Bill); Krstina, J.; Le, T. P. T.; Moad, G.; Postma, A.; Rizzardo, E.; Thang, S. H. *Macromolecules* **2003**, *36*, 2256−2272.

MA0358428